

Article

In-Situ Reaction Method to Synthesize Constant Solid-State Composites as Phase Change Materials for Thermal Energy Storage

Bo Yang ^{*}, Yang Liu, Wenjie Ye, Qiyang Wang, Xiao Yang and Dongmei Yang

Joint Laboratory of Regional Energy Internet Technology and Application of State Grid Corporation, State Grid Electric Power Research Institute, Nanjing 211106, China; liuyang9@sgepri.sgcc.com.cn (Y.L.); yewenjie@sgepri.sgcc.com.cn (W.Y.); wangqiyang@sgepri.sgcc.com.cn (Q.W.); yangxiao1@sgepri.sgcc.com.cn (X.Y.); yangdongmei@sgepri.sgcc.com.cn (D.Y.)

* Correspondence: yangbo3@sgepri.sgcc.com.cn; Tel.: +86-15850742612

Abstract: The encapsulation and heat conduction of molten salt are very important for its application in heat storage systems. The general practice is to solidify molten salt with ceramic substrate and enhance heat conduction with carbon materials, but the cycle stability is not ideal. For this reason, it is of practical significance to study heat storage materials with a carbon-free thermal conductive adsorption framework. In this paper, the in-situ reaction method was employed to synthesize the constant solid-state composites for high-temperature thermal energy storage. AlN is hydrolyzed and calcined to form h-Al₂O₃ with a mesoporous structure to prevent the leakage of molten eutectic salt at high temperature. Its excellent thermal conductivity simultaneously improves the thermal conductivity of the composites. It is found that 15CPCMs prepared with 15% water addition have the best thermal conductivity (4.928 W/m·K) and mechanical strength (30.2 MPa). The enthalpy and the thermal storage density of 15CPCMs are 201.4 J/g and 1113.6 J/g, respectively. Due to the excellent leak-proof ability and lack of carbon materials, the 15CPCMs can maintain almost no mass loss after 50 cycles. These results indicate that 15CPCMs have promising prospects in thermal storage applications.

Keywords: thermal energy storage; in-situ reaction; 15CPCMs; thermophysical properties



Citation: Yang, B.; Liu, Y.; Ye, W.; Wang, Q.; Yang, X.; Yang, D. In-Situ Reaction Method to Synthesize Constant Solid-State Composites as Phase Change Materials for Thermal Energy Storage. *Materials* **2021**, *14*, 6032. <https://doi.org/10.3390/ma14206032>

Academic Editors: Francisco de Paula Montero Chacón and Juan Carlos Serrano-Ruiz

Received: 1 September 2021

Accepted: 12 October 2021

Published: 13 October 2021

Publisher's Note: MDPI stays neutral with regard to jurisdictional claims in published maps and institutional affiliations.



Copyright: © 2021 by the authors. Licensee MDPI, Basel, Switzerland. This article is an open access article distributed under the terms and conditions of the Creative Commons Attribution (CC BY) license (<https://creativecommons.org/licenses/by/4.0/>).

1. Introduction

With the rise of integrated energy in recent years, thermal energy storage systems have played an increasingly vital role in energy coupling to ensure the safe, economic and efficient supply of energy [1,2]. As a key component, thermal storage materials have received a great deal of attention from researchers [3–5]. Obviously, the most valuable and promising materials are based on latent thermal storage using phase change materials (PCMs) [6–8], which have a high heat storage density and constant temperature during the charge/discharge process [9,10]. Compared with hydrated salt and their mixture, molten salt is more attractive with the advantages of low subcooling, high melting temperature and high phase stability, which offer more potential for applications in solar thermal uses, waste heat recovery, steam production and so on [11,12].

However, limited by its low thermal conductivity, insurmountable thermal expansion and corrosion, there are still many difficulties for molten salt in practical use as a heat storage material [13,14]. To date, many efforts have been made to solve these problems, which can be summarized as follows: forming a skeleton by the use of chemical and physical compatible ceramic materials and enhancing the heat conductivity by the addition of thermal conductivity materials [15–18]. Awad [19] prepared nanosalts by dispersing nanoparticles in nitrate, whose total heat storage increased by 6% due to the formation of an interface layer. Porous Si₃N₄ ceramic acted as a heat-conducting skeleton material to

prepare shape-stabilized phase change material in Wang's work [15], and the finished product showed good thermal conductivity and cyclic stability. By inserting the mixture of salt into the cavities of diatomite, Miliozzi [20] fabricated solar salt/diatomite composite PCMs, which showed increased thermal and mechanical properties without any phase change material leakage. A shape-stable $\text{Na}_2\text{CO}_3\text{-K}_2\text{CO}_3/\text{CFA}/\text{EG}$ composite phase change material was developed by Wang [21]. It was found that the addition of expanded graphite has little effect on the heat storage density but can greatly improve the thermal conductivity ($3.182 \text{ W/m}\cdot\text{K}$) of the composites. Sang [22] studied composite PCMs based on MgO and ternary carbonate, and the results showed that when the mass ratio of MgO and ternary carbonate was 1:1, the composite PCMs had the best energy storage performance and thermophysical properties. Ye [23] prepared CPCMs with MgO and multi-layer carbon nanotubes as a ceramic framework and thermal agent, respectively. The study found that the overall structure of the material is stable, and the thermal conductivity is significantly enhanced with increased amounts of multi-layer carbon nanotubes. The wettability of the molten salt on the ceramic and carbon materials was also studied [24], showing that the amount of carbon materials significantly affected the microstructure and properties of the composites. Li [25] employed a milling and sintering approach to fabricate MgO-based PCMs with different particle sizes and densities of MgO. They found that light and smaller MgO particles could provide better thermophysical and mechanical properties for PCMs and that graphite loading is the important factor affecting the thermal conductivity.

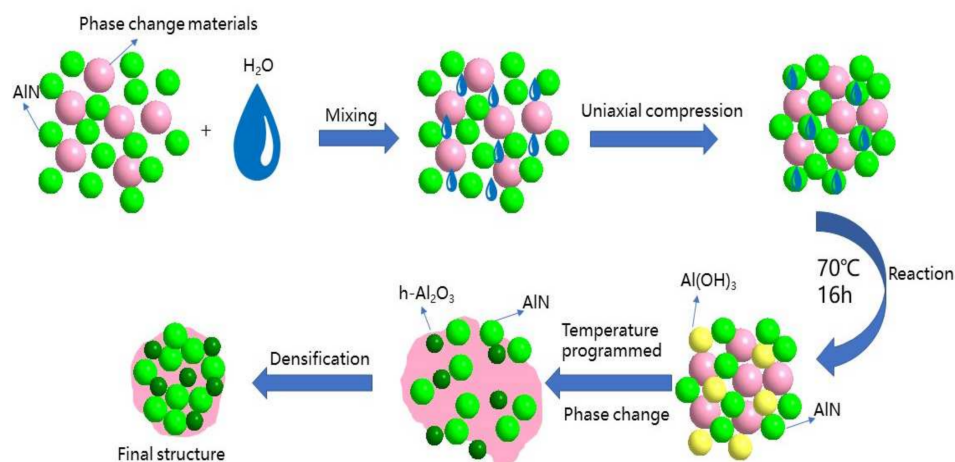
Though the research work in the above literature has solved the problems of the shaping and heat conduction of PCMs to a certain extent, there are still some defects left: the pure ceramic ($<36 \text{ W/m}\cdot\text{K}$) framework has good molten salt fixation ability but poor thermal conductivity [23], while carbon materials have good thermal conductivity but poor high temperature stability and molten salt dispersion [26]. Herein, an in-situ reaction method is proposed to synthesize constant solid-state CPCMs. AlN powder (up to $180 \text{ W/m}\cdot\text{K}$) is used and partially hydrolyzed to form a ceramic framework, while the remaining powder acts as a thermal conductive material. In this way, a uniform and continuous thermal conduction skeleton of a ceramic matrix is formed, which means that the CPCMs can obtain higher thermal conductivity and cycle stability.

2. Materials and Methods

2.1. Raw Materials and Sample Preparation

Constant solid-state composites were obtained via an in-situ reduction method, as described in Scheme 1. The PCMs used in this study were carbonate-based eutectic salt made from a mixture of Li_2CO_3 (AR, Aladdin reagent Co., Ltd., Shanghai, China) and Na_2CO_3 (AR, Aladdin reagent Co., Ltd., Shanghai, China) with a mole ratio of 1:1. Ceramic powder (AlN, purity $> 98\%$, Liaoning Desheng special ceramics manufacturing Co., Ltd., Tieling, China), with a particle size of about $10 \mu\text{m}$, was chosen to produce the thermal conductive reinforced framework. All these raw materials were used without further purification.

To synthesize the composites, a certain amount of eutectic salt and AlN powder was mixed by the method of high-speed shear. Then, deionized water was added into the mixture homogeneously to prepare composite powder, which was shaped under a uniaxial press of 30 MPa for 3 min. The precursor was sealed and heated for 16 h at a temperature of $70 \text{ }^\circ\text{C}$ to ensure full reaction. In this way, green bulks were obtained. Finally, the green bulks were sintered by the following heating procedure: they were heated to $105 \text{ }^\circ\text{C}$ at $5 \text{ }^\circ\text{C}/\text{min}$ and held for 1 h; raised to $300 \text{ }^\circ\text{C}$ at $10 \text{ }^\circ\text{C}/\text{min}$ and held for 2.5 h; raised to $550 \text{ }^\circ\text{C}$ at $5 \text{ }^\circ\text{C}/\text{min}$ and held for 2 h; and finally cooled down to room temperature. The contrast samples were prepared by using Al_2O_3 nano powder and flake graphite as skeleton and thermal conductivity materials, respectively.



Scheme 1. The synthesis process of the constant solid-state CPCMs.

2.2. Material Characterization

The phase structures of materials were characterized by X-ray diffraction (XRD) (D8 advance, Bruker, Karlsruhe, Germany) with Cu K α radiation ($\lambda = 1.5418 \text{ \AA}$, 40 kV, 40 mA). The morphologies were observed by scanning electron microscopy (SEM) (Nova Nano 450, FEI, Hillsboro, OR, USA) with energy dispersive X-ray analysis (EDS, Octane Super, EDAX, Pleasanton, CA, USA). The chemical state of materials was investigated by X-ray photoelectron spectroscopy (XPS) (K-Alpha 1063, Thermo Scientific, Waltham, MA, USA). The specific surface area and pore volume of the materials were analyzed with the BET method (ASAP 2460, Micromeritics, Norcross, GA, USA). The measurements of melting temperature, latent heat and thermal stability were performed with a simultaneous thermal analyzer (TG-DSC) (STA449F3, Netzsch, Waldkraiburg, Germany) from room temperature to 600 °C at a heating rate of 10 °C/min under air. The specific heat capacity of samples was tested by the sapphire method on the same instrument. The thermal conductivity of the samples was detected by a thermal constant analyzer (TPS 2500S, Hot Disk, Uppsala, Sweden) at room temperature. The mechanical strength of the CPCMs was measured by the electronic universal material testing machine (CMT4202, Shenzhen Xinsansi Material Test Co. Ltd., Shenzhen, China).

2.3. Thermal Cycling Test

To obtain the thermal cycling performance of the CPCMs, all of the samples were loaded into corundum crucibles and then placed into the muffle furnace. In the test, the temperature was raised to 600 °C at a heating rate of 10 °C/min for 1 h to ensure the completion of the phase change process and then downed with the furnace. This was recorded as a cycle. A total of 50 cycles were carried out and the mass data were recorded every 5 times.

3. Results and Discussion

3.1. Mechanical Strength and Thermal Conductivity of CPCMs

Figure 1 shows the appearances of the CPCMs made with different levels of water addition and the contrast sample. As shown in Figure 1a,b, there was a serious leakage for 0CPCMs and 5CPCMs due to the inability to produce enough skeleton materials. Though 10% water addition can allow the 10CPCMs to be shaped, the escape of phase change materials at high temperature cannot be prevented. For CPCMs made with more than 15% water addition, they have perfect appearances without any leakage. As above, this indicates that with at least 15% water addition, the produced CPCMs can wrap the eutectic salt. The contrast sample exhibits an excellent appearance, similar to that of 15CPCMs and 20CPCMs, which shows the good adsorption capacity of nano Al₂O₃.

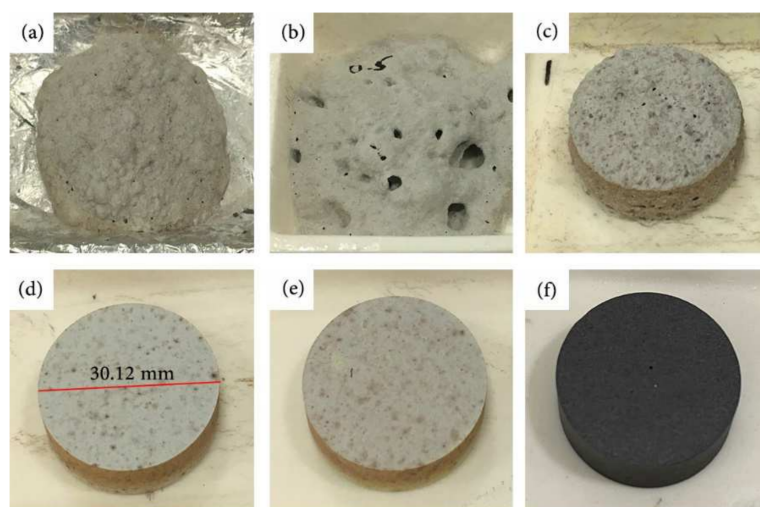


Figure 1. Photographs of the CPCM made with different water addition: (a) 0%, (b) 5%, (c) 10%, (d) 15%, and (e) 20% water and (f) the contrast sample.

The physical parameters of density, mechanical strength and thermal conductivity are of great importance to CPCM for practical use. Thus, the stable samples were chosen for further study, as shown in Table 1. Comparing 15CPCMs with 20CPCMs, it can be found that water addition has an obvious effect on the density, which can be attributed to the hydrolysis of AlN powder. As the control agent of reaction, the amount of water determines the rate of reaction and the amount of product and then affects the density of CPCM. The density is closely related to mechanical strength and heat conduction, so the three technical indicators of 15CPCMs are higher than 20CPCMs. Due to the thermal inertia and fluffiness of nano Al₂O₃, although graphite has good thermal conductivity and compaction density, the contrast sample still displays worse performance than 15CPCMs.

Table 1. Density, mechanical strength and thermal conductivity of the composite materials.

Name	ρ (g/cm ³)	P (MPa)	K (W/m·K)
15CPCMs	1.86	30.2	4.928
20CPCMs	1.73	26.3	4.149
Contrast sample	1.69	18.5	4.465

3.2. Chemical Compatibility and Microstructures of CPCM

Figure 2 shows the XRD patterns of 15CPCMs, eutectic salt, AlN and h-Al₂O₃, where h-Al₂O₃ represents the result of AlN after hydrolysis and calcination. The eutectic salt was made from Li₂CO₃-Na₂CO₃ according to the mole ratio of 1:1, which matches well with standard LiNaCO₃ (JCPDS No. 34-1193). As shown in Figure 2a, the characteristic peaks of eutectic salt, AlN and h-Al₂O₃ are all observed in the XRD pattern of 15CPCMs, which proves that part of AlN reacts to generate h-Al₂O₃ during the preparation process. Besides, no new peaks could be detected, indicating that there were no chemical reactions among eutectic salt, AlN and h-Al₂O₃. It is worth mentioning that the crystallinity of h-Al₂O₃ is poor according to the broad band of the XRD pattern.

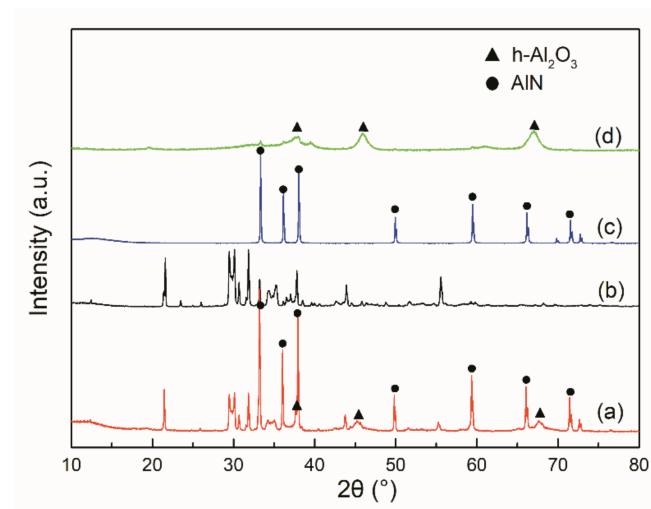


Figure 2. XRD patterns of (a) 15CPCMs, (b) eutectic salt, (c) AlN and (d) $h\text{-Al}_2\text{O}_3$.

The elemental compositions of the 15CPCMs were examined by XPS analysis. As shown in Figure 3a, there are five distinct peaks in the wide-scan XPS spectrum, illustrating the existence of C, N, Al and O atoms. The group peaks near 979.7 eV are the auger electron spectra of oxygen, which is the KLL series. The C1s region consists of two strong peaks at 285.0 eV and 289.4 eV, which can be attributed to sp^2 -bonded carbon and MCO_3 , indicating that the composites contain carbonate. The N1s core level spectrum at 397.1 eV and 399.4 eV is related to AlN and the binding energy of O1s at 531.1 eV indicates the presence of Al_2O_3 . Furthermore, the binding energy peak at 73.8 eV represents the Al bonded to N, which is consistent with the detection of N1s. This testing result reveals that the components of 15CPCMs include AlN, Al_2O_3 and carbonate.

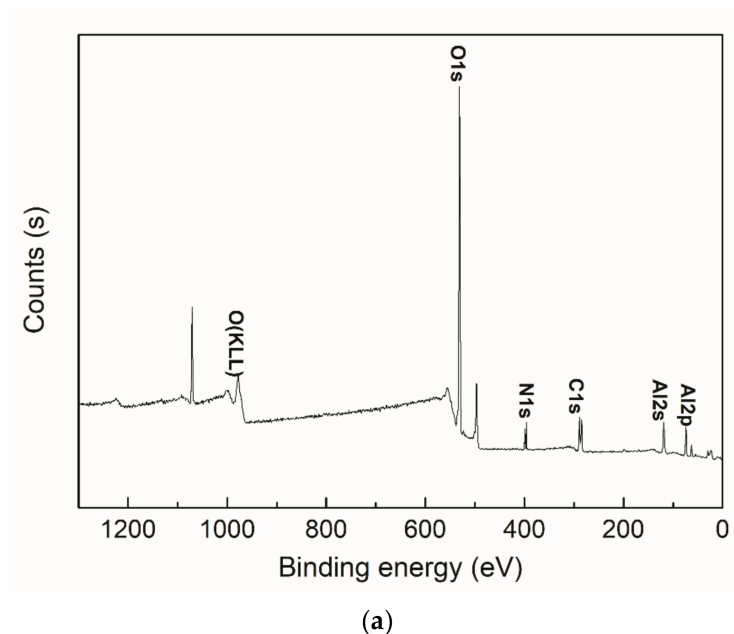


Figure 3. Cont.

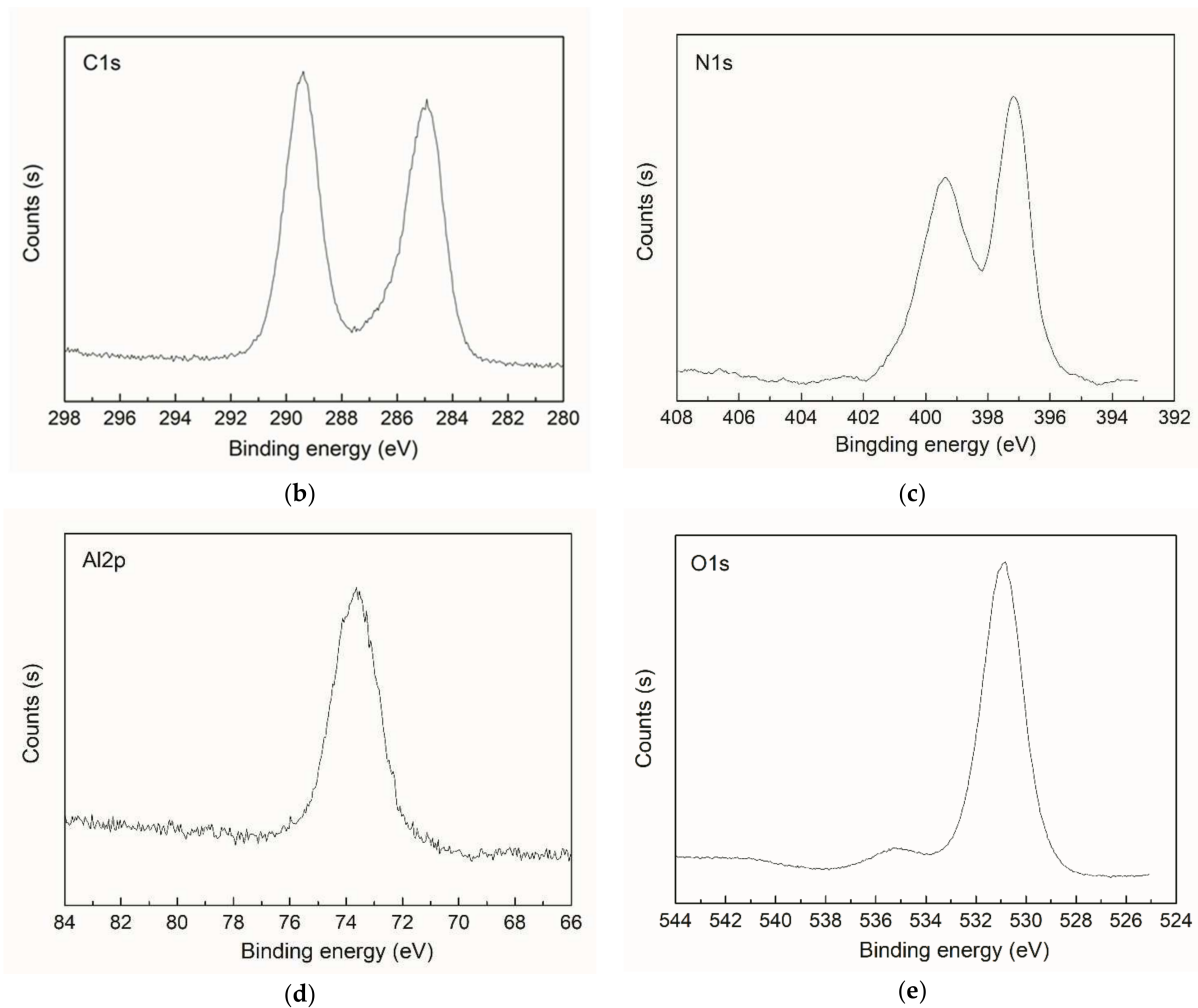


Figure 3. Wide-scan XPS spectrum of 15CPCMs (a). High-resolution scan for (b) C1s, (c) N1s, (d) Al2p and (e) O1s core levels.

Figure 4d gives the morphology of h-Al₂O₃, which presents a flower-like appearance with the petals size below 1 μm , and many pores are formed among the petals to accommodate the phase change materials. Thanks to this microstructure, the upper surface and section of 15CPCMs show a dense appearance without holes (Figure 4a,b), indicating that there is no eutectic salt volatilization at high temperature. From Figure 4e, it can be further observed that the eutectic salt is wrapped by the h-Al₂O₃. Compared to this, AlN shows a smooth appearance with no pores (Figure 4c). Therefore, the capillary force provided by the molten salt is insufficient to hold the AlN together [24], and the 0CPCMs prepared with it cannot be formed after sintering.

The N₂ adsorption and desorption were carried out for h-Al₂O₃ to evaluate the permanent porosity. The h-Al₂O₃ exhibits the reversible type IV isotherm, which is one of the main characteristics of mesoporous materials (Figure 5). The surface area of h-Al₂O₃ was calculated to be 58 m²g⁻¹ using the Brunauer–Emmett–Teller (BET) model. The pore size distribution of h-Al₂O₃ can also be observed in Figure 5, showing peak pore sizes of 5 nm and 13 nm. Obviously, this is within the size range of mesopores, indicating that the material has a mesoporous structure. This is the reason why the 15CPCMs made with h-Al₂O₃ exhibit excellent performance.

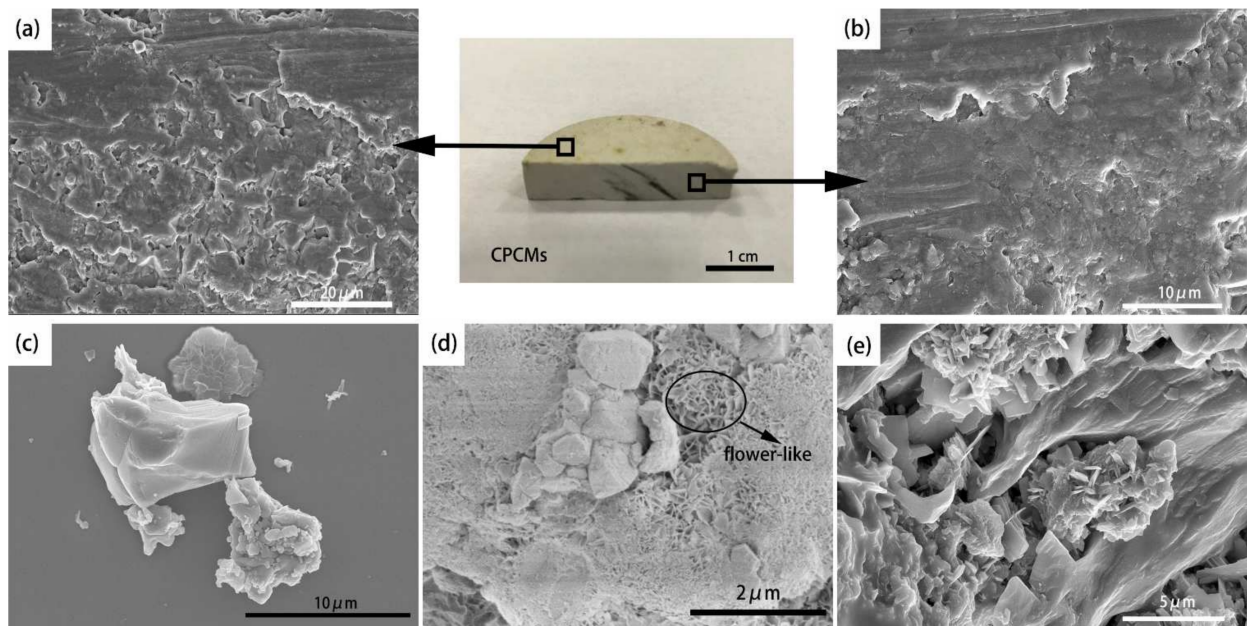


Figure 4. SEM images of 15CPCMs and components: (a) upper surface, (b,e) section of 15CPCMs, (c) AlN and (d) h-Al₂O₃.

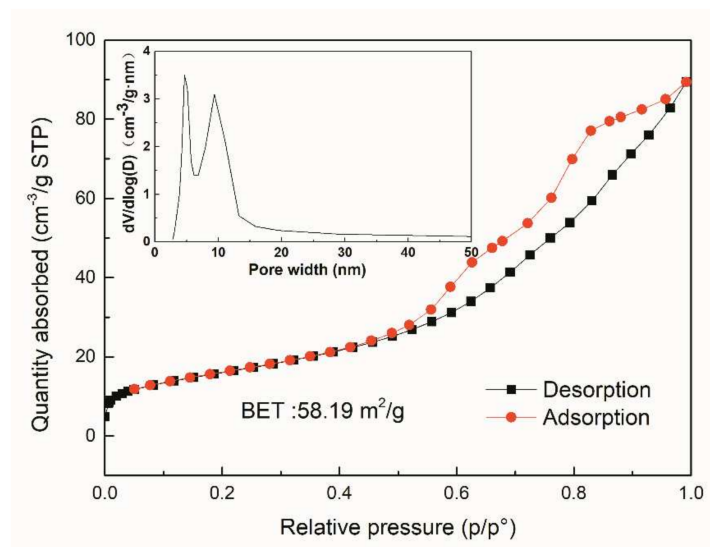


Figure 5. N₂ adsorption–desorption isotherms and pore size distribution of h-Al₂O₃.

3.3. Thermophysical Properties of the Composites

The TG–DSC curves for the eutectic salt and 15CPCMs after 1 cycle and 50 cycles are given in Figure 6. It can be seen from the TG curves that there is an obvious mass loss for eutectic salt at 600 °C, indicating that although the decomposition temperature of a single component is not reached, the eutectic salt has begun to volatilize at this temperature, while the 15CPCMs have almost no mass loss at 600 °C, which proves that the formation of capillary force and surface tension by the mesoporous structure is of positive significance for the immobilization of liquid eutectic salt. From the DSC curves, the enthalpy of eutectic salt is 348.5 J/g, while the enthalpy of 15CPCMs is 201.4 J/g, which is about 57.8% of the former. The encapsulation amount of eutectic salt is higher than that reported in the literature [22,24]. Even after 50 thermal cycles, the enthalpy of 15CPCMs is hardly changed, which illustrates their good thermal stability. The melting temperature peak of 15CPCMs

is ~ 2.4 °C lower than that of eutectic salt, which may be associated with the surface energy differences. This is consistent with the results of Li's research [25].

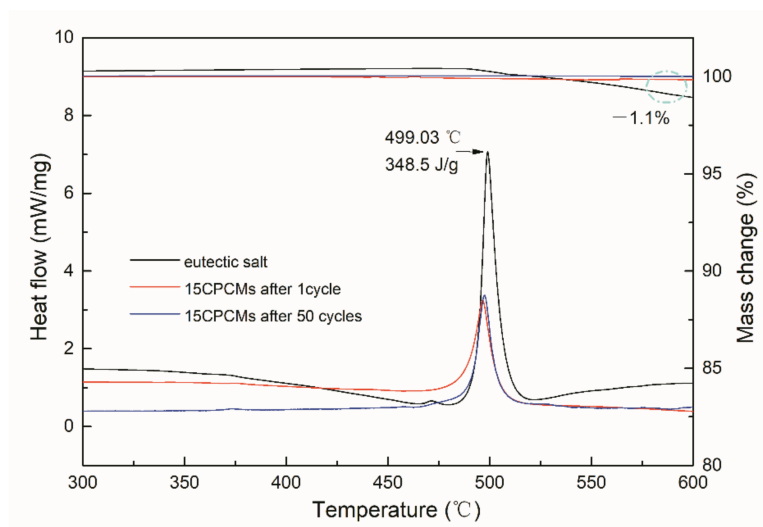


Figure 6. TG-DSC curves for eutectic salt and 15CPCMs after 1 cycle and 50 cycles.

Thermal storage density is an important parameter to measure the practicability of thermal storage materials. To calculate the thermal storage density, it is necessary to consider both the latent heat of the eutectic salt and the sensible heat of the composite material. The calculation formula for thermal storage density is shown in Equation (1) in the temperature range from T_0 to T_1 :

$$Q = \Delta H_{lat} + \int_{T_0}^{T_1} C_p d_t \quad (1)$$

where Q is the total thermal energy stored in the composites per unit mass. ΔH_{lat} stands for the latent heat of molten salts and C_p represents the specific heat capacity of the composites, which are all detected by the simultaneous thermal analyzer. Figure 7 gives the specific heat capacity curve of 15CPCMs from 200 °C to 600 °C. Therefore, within this service temperature range, the heat storage density value of 15CPCMs is as high as 1113.6 J/g. Compared to the ternary carbonates/MgO composites obtained by Sang [22], whose thermal storage density is 781.4 kJ/kg, the result is obviously more attractive.

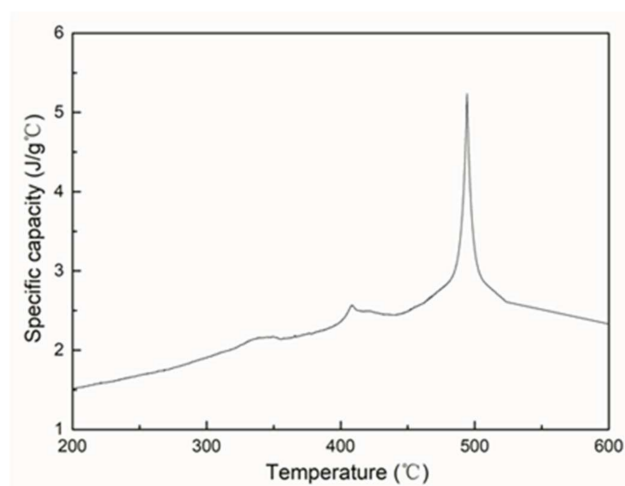


Figure 7. Specific heat capacity curve of 15CPCMs.

Figure 8 gives the mass change of 15CPCMs and the contrast sample. The mass of 15CPCMs is almost unchanged after 50 cycles, indicating that the eutectic salt does not leak out from the ceramic matrix heat conduction skeleton, which can be proved by Figure 9c,d. This is consistent with the TG-DSC test results, and the enthalpy is roughly equal before and after cycling. However, the contrast sample loses about a quarter of its weight after 50 cycles. The reason for this can be attributed to the following: firstly, the continuous oxidation of graphite causes weight loss; secondly, the pores generated after graphite oxidation make the eutectic salt easy to volatilize, resulting in weight loss. These can be proved by Figure 9a,b. After 50 cycles, the contrast sample turns white due to the oxidation of graphite and presents an unsmooth and porous morphology.

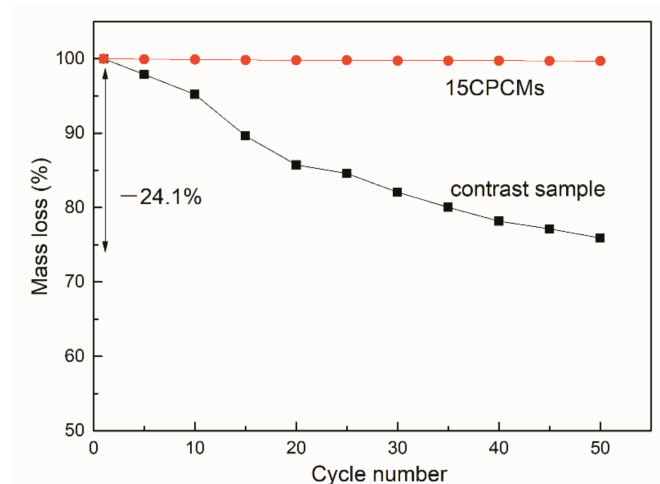


Figure 8. Weight loss curves of 15CPCMs and contrast sample.

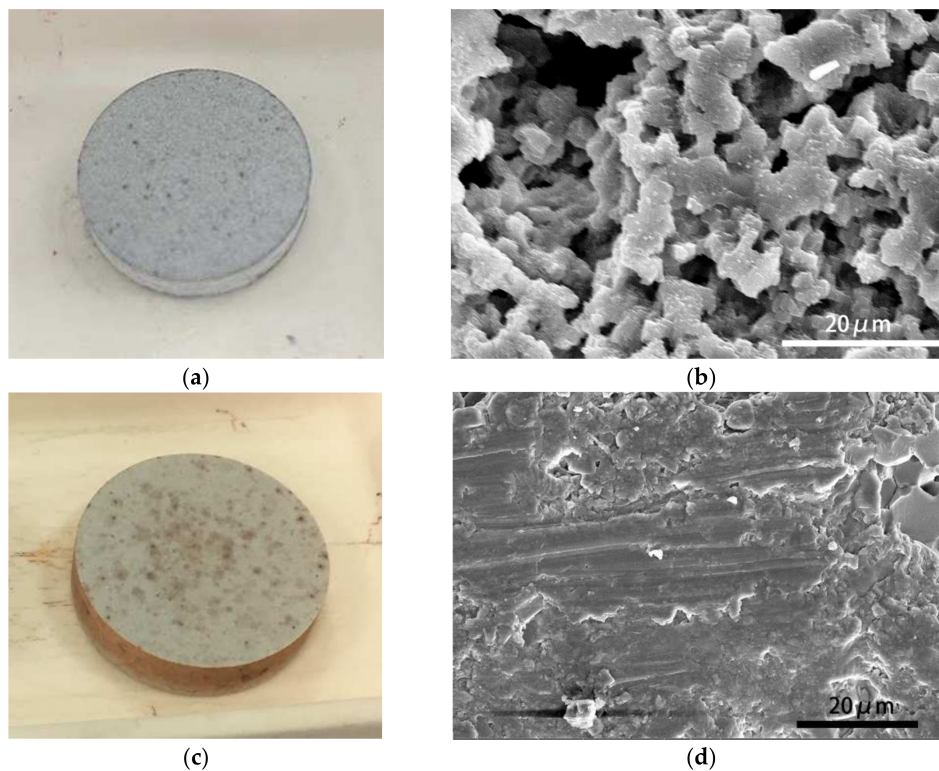


Figure 9. Morphology of contrast sample and 15CPCMs after 50 cycles: (a) photograph of contrast sample, (b) SEM image of contrast sample, (c) photograph of 15CPCMs, (d) SEM image of 15CPCMs.

4. Conclusions

Constant solid-state CPCMs with a carbon-free thermal conductive adsorption framework were prepared by an in-situ reaction method. In the CPCMs, carbonate-based eutectic salt (LiNaCO_3) functions as the PCMs, while AlN serves as a thermal conducting material and generates $\text{h-Al}_2\text{O}_3$ through hydrolysis and calcination, which acts as a skeleton material for shape stabilization. We found that 15% of water addition can allow CPCMs to form and obtain the best performance, showing a mechanical strength of 30.2 MPa and a thermal conductivity of 4.928 W/m·K. Further study reveals that $\text{h-Al}_2\text{O}_3$ is a mesoporous structure that can produce enough capillary force and surface tension to prevent the leakage of molten eutectic salt at high temperature, which is the reason why the 15CPCMs exhibit excellent performance. The thermophysical test results show that the enthalpy and the thermal storage density of 15CPCMs are 201.4 J/g and 1113.6 J/g, respectively. After 50 cycles, the 15CPCMs have almost no mass loss and exhibit excellent thermal stability, which is much better than that of carbon-containing composites. All these factors prove that 15CPCMs are a promising high-temperature thermal energy storage material.

Author Contributions: Conceptualization, B.Y.; Data curation, B.Y., Y.L. and Q.W.; Formal analysis, B.Y. and Y.L.; Funding acquisition, X.Y.; Resources, W.Y. and Q.W.; Supervision, D.Y.; Validation, Y.L., W.Y. and X.Y.; Writing—original draft, B.Y.; Writing—review & editing, B.Y. All authors have read and agreed to the published version of the manuscript.

Funding: This research was funded by the Science and Technology Project in Jiangsu Province (Grant No. BE2020081 and BZ2019057).

Institutional Review Board Statement: Not applicable.

Informed Consent Statement: Not applicable.

Data Availability Statement: Available upon request from the corresponding author.

Conflicts of Interest: The authors declare no conflict of interest.

References

1. Liu, X.; Wu, J.; Jenkins, N. Combined analysis of electricity and heat networks. *Appl. Energy* **2016**, *162*, 1238–1250. [[CrossRef](#)]
2. Wei, H.; Xie, X.; Li, X.; Lin, X. Preparation and characterization of capric-myristic-stearic acid eutectic mixture/modified expanded vermiculite composite as a form-stable phase change material. *Appl. Energy* **2016**, *178*, 616–623. [[CrossRef](#)]
3. Qiu, Z.; Ma, X.; Zhao, X.; Wright, A. Micro-encapsulated phase change material (MPCM) slurries: Characterization and building applications. *Renew. Sustain. Energy Rev.* **2017**, *77*, 246–262. [[CrossRef](#)]
4. Cunha Da, J.-P.; Eames, P. Thermal energy storage for low and medium temperature applications using phase change materials—a review. *Appl. Energy* **2016**, *177*, 227–238. [[CrossRef](#)]
5. Nkhonjera, L.; Bello-Ochende, T.; John, G.; King'onde, C.-K. A review of thermal energy storage designs, heat storage materials and cooking performance of solar cookers with heat storage. *Renew. Sustain. Energy Rev.* **2017**, *75*, 157–167. [[CrossRef](#)]
6. Zhang, P.; Xiao, X.; Ma, Z.W. A review of the composite phase change materials: Fabrication, characterization, mathematical modeling and application to performance enhancement. *Appl. Energy* **2016**, *165*, 472–510. [[CrossRef](#)]
7. Nomura, T.; Akiyama, T. High-temperature latent heat storage technology to utilize exergy of solar heat and industrial exhaust heat. *Int. J. Energy Res.* **2017**, *41*, 240–251. [[CrossRef](#)]
8. Nomura, T.; Sheng, N.; Zhu, C.; Saito, G.; Hanzaki, D.; Hiraki, T. Microencapsulated phase change materials with high heat capacity and high cyclic durability for high-temperature thermal energy storage and transportation. *Appl. Energy* **2017**, *188*, 9–18. [[CrossRef](#)]
9. Zhang, X.-G.; Wen, R.-L.; Tang, C.; Wu, B.-G.; Huang, Z.-H.; Min, X.; Huang, Y.-T.; Liu, Y.-G.; Fang, M.-H.; Wu, X.-W. Thermal conductivity enhancement of polyethylene glycol/expanded perlite with carbon layer for heat storage application. *Energy Build* **2016**, *130*, 113–121. [[CrossRef](#)]
10. Qureshi, Z.-A.; Ali, H.-M.; Khushnood, S. Recent advances on thermal conductivity enhancement of phase change materials for energy storage system: A review. *Int. J. Heat Mass Transf.* **2018**, *127*, 838–856. [[CrossRef](#)]
11. Ge, Z.-W.; Li, Y.-L.; Li, D.-C.; Sun, Z.; Jin, Y.; Liu, C.-P. Thermal energy storage: Challenges and the role of particle technology. *Particuology* **2014**, *15*, 2–8. [[CrossRef](#)]
12. Krasna, M.; Klemencic, E.; Kutnjak, Z.; Kralj, S. Phase-changing materials for thermal stabilization and thermal transport. *Energy* **2018**, *162*, 54–63. [[CrossRef](#)]
13. Wu, Y.-T.; Ren, N.; Wang, T.; Ma, C.-F. Experimental study on optimized composition of mixed carbonate salt for sensible heat storage in solar thermal power plant. *Sol. Energy* **2011**, *85*, 1957–1966. [[CrossRef](#)]

14. Han, D.; Lougou, B.-G.; Xu, Y.-T.; Shuai, Y.; Huang, X. Thermal properties characterization of chloride salts/nanoparticles composite phase change material for high-temperature thermal energy storage. *Appl. Energy* **2020**, *264*, 114674. [[CrossRef](#)]
15. Wang, H.-R.; Ran, X.-F.; Zhong, Y.J.; Lu, L.-Y.; Lin, J.; He, G.; Wang, L.; Dai, Z.-M. Ternary chloride salt-porous ceramic composite as a high-temperature phase change material. *Energy* **2022**, *238*, 121838. [[CrossRef](#)]
16. Giovanni, S.-S.; Valerio, T.; Anna, C.-T.; Raffaele, L.; Emiliana, M.; Annarita, S.; Natale, C.; Mauro, C.; Tiziano, D.; Anna, D.-L. High-Temperature Chloride-Carbonate Phase Change Material: Thermal Performances and Modelling of a Packed Bed Storage System for Concentrating Solar Power Plants. *Energies* **2021**, *14*, 5339.
17. Gil, A.; Peiró, G.; Oró, E.; Cabeza, L.F. Experimental analysis of the effective thermal conductivity enhancement of PCM using finned tubes in high temperature bulk tanks. *Appl. Therm. Eng.* **2018**, *142*, 736–744. [[CrossRef](#)]
18. Gimenez-Gavarrell, P.; Fereres, S. Glass encapsulated phase change materials for high temperature thermal energy storage. *Renew. Energy* **2017**, *107*, 497–507. [[CrossRef](#)]
19. Awad, A.; Navarro, H.; Ding, Y.-L.; Wen, D.-S. Thermal-physical properties of nanoparticle-seeded nitrate molten salts. *Renew. Energy* **2018**, *120*, 275–288. [[CrossRef](#)]
20. Miliuzzi, A.; Chieruzzi, M.; Torre, L. Experimental investigation of a cementitious heat storage medium incorporating a solar salt/diatomite composite phase change material. *Appl. Energy* **2019**, *250*, 1023–1035. [[CrossRef](#)]
21. Wang, T.-Y.; Wang, K.-C.; Ye, F.; Ren, Y.-X.; Xu, C. Characterization and thermal properties of a shape-stable Na₂CO₃-K₂CO₃/coal fly ash/expanded graphite composite phase change materials for high-temperature thermal energy storage. *J. Energy Storage* **2021**, *33*, 102123. [[CrossRef](#)]
22. Sang, L.; Li, F.; Xu, Y. Form-stable ternary carbonates/MgO composite material for high temperature thermal energy storage. *Sol. Energy* **2019**, *180*, 1–7. [[CrossRef](#)]
23. Ye, F.; Ge, Z.-W.; Ding, Y.-L.; Yang, J. Multi-walled carbon nanotubes added to Na₂CO₃/MgO composites for thermal energy storage. *Particuology* **2013**, *15*, 56–60. [[CrossRef](#)]
24. Ge, Z.-W.; Ye, F.; Cao, H.; Leng, G.-H.; Qin, Y.; Ding, Y.-L. Carbonatesalt-based composite materials for medium and high temperature thermal energy storage. *Particuology* **2014**, *15*, 77–81. [[CrossRef](#)]
25. Li, C.; Li, Q.; Lin, C.; Feng, J.; Zhao, Y.-Q.; Liu, C.-P.; Xiong, Y.-X.; Chang, C.; Ding, Y.-L. MgO based composite phase change materials for thermal energy storage: The effects of MgO particle density and size on microstructural characteristics as well as thermophysical and mechanical properties. *Appl. Energy* **2019**, *250*, 81–91. [[CrossRef](#)]
26. Pincemin, S.; Olives, R.; Py, X.; Christ, M. Highly conductive composites made of phase change materials and graphite for thermal storage. *Sol. Energy Mater. Sol. Cells* **2008**, *92*, 603–613. [[CrossRef](#)]